7ICMSNSE-39

New Exploration on TMSR: Modelling and Simulation

Shengyi Si Qichang Chen Hua Bei Jinkun Zhao
Shanghai Nuclear Engineering Research & Design Institute
No.29 Hongcao Road, Shanghai 200233, China
ssy@snerdi.com.cn

Abstract

A tightly coupled multi-physics model for MSR (Molten Salt Reactor) system involving the reactor core and the rest of the primary loop has been developed and employed in an in-house developed computer code TANG-MSR. In this paper, the computer code is used to simulate the behavior of steady state operation and transient for our redesigned TMSR. The presented simulation results demonstrate that the models employed in TANG-MSR can capture major physics phenomena in MSR and the redesigned TMSR has excellent performance of safety and sustainability.

Keywords: Multi-physics model, Redesigned TMSR, Depletion, Steady State, Transient

1. Introduction

Molten Salt Reactor (MSR), which employs liquid salt as fuel and solid graphite as moderator, has been recognized as one of the most promising reactor types satisfying the performance requirements of Next Generation Nuclear Power Plant, such as Sustainability, Economy, Safety and Non-proliferation [1]. There have been a lot of conceptual MSR designs presented during past decades [2-6]. Most of these concepts are the variants evolved from the Molten-Salt Breeder Reactor (MSBR) based on 'Single Fluid Molten Fluoride Fuel'[7,8], which was originated from Molten-Salt Reactor Program, Oak Ridge National Laboratory (ORNL), USA among 1950~1976. TMSR (Thorium Molten Salt Reactor) is just one of these variants which employ liquid thorium-based fuel salt and solid moderator.

Schematically, MSR is quite different from other reactors employing solid fuel and liquid coolant. Firstly, the fuel salt act as both fuel and coolant, therefore, the Neutronics and Thermal-hydraulics are tightly coupled with each other in MSR; secondly, the flowing fuel exist in not only reactor core but also the plenums, pipes and main components (HX, Pump), therefore, the fuel depletion and delayed neutron precursors distribution shall undergo completed course in MSR; thirdly, Online fuel processing (fission gas separation, noble metal plate out, feeding and extracting) shall directly disturb the fuel compositions in MSR, therefore, the behaviour of fuel depletion and isotopes inventory variation shall be also quite complicated. In one word, the modelling and simulation for MSR is quite different from those reactors employing solid fuel and liquid coolant.

There have been a lot of efforts devoted by different authors to model and simulate MSR steady state and/or transients with various assumptions [9-21]. Generally, the features of these efforts can be summarized as follows:

- Most of these efforts are based on existing codes, originally for the reactor core employing solid fuel, specially with extension to model flowing fuel in the core; whereas, these models mainly focus on reactor core without explicit approaches for the rest of the primary loop, such as pipes, HX and pumps, therefore, the travelling time sharing of flowing fuel in each stop (core, plenums, pipes, HX, etc.) of the primary loop, is not estimated by code with

consistent algorithm but some prescribed input data, whereas, it is crucial for the estimation of delayed neutron loss, precursor distribution in 3D-core and isotopes' depletion.

- Some of these efforts mainly aim at investigating the transient behaviours without comprehensive modelling for depletion effect during normal operation, especially for the online fuel processing (fission gas separation, noble metal plate out, feeding and extracting).
- Some of these efforts are based on 0D, 1D or synthetic 2D+1D model with homogenous cross section approach and prescribed uniform velocity field, which ignore the spatial effects of density, temperature and velocity of fuel and/or moderator.

In order to have a deeper insight into the steady state and transient characteristics of TMSR for both initial state and depleted state, we developed a comprehensive multi-physics model for TMSR system involving the reactor core and the rest of the primary loop. As for the Neutronics model, we solve 3D steady state and/or kinetic multi-group neutron diffusion equations with heterogeneous cross sections, which are the functions of fuel density/ temperature and moderator temperature. The thermal-hydraulic models covered the primary loop of the TMSR. The fuel temperature and mass density for all the fuel channels in active core are estimated by solving energy balance equations, the heat transfer within solid moderator is taken into account by solving heat conduction equation, and the mass flow rates for each fuel channel are estimated by solving momentum (pressure drop) balance equations. As a result, the 3D temperature field and 3D fluid field (density and velocity) of liquid fuel in active core can be explicitly calculated. The fuel flowing through the rest of the primary loop, such as plenums, pipes and HX, is modelled, so that travelling time and precursor density in each parts of the primary loop can be estimated explicitly. A dedicated depletion model is adopted to track the isotope composition evolution due to the effect of depletion in core and decay in primary loop, and also the effect of online fuel processing, such as fission gas separation, noble metal plate out, feeding and extracting, therefore, it is easy to investigate the characteristics of TMSR steady operation and transient for both initial core and depleted core.

The paper introduces the models employed in our in-house developed compute code TANG-MSR, which is a special TANG version for TMSR simulation and analysis. Some simulation results shall be presented and discussed.

2. TMSR System and Modelling

2.1 System Description

The TMSR system we simulated is similar to the ORNL's MSBR [7], which employs Single Fluid Molten-Salt as fuel and graphite as moderator and in which the fuel composition is 71.7%LiF -16BeF_2- 12%ThF_4- 0.3%UF_4. Since the recent re-evaluations to MSBR [22, 23] have revealed that the MSR with this lattice design might present positive power coefficient and may be uncontrollable under normal operation and transient, we have redesigned the lattice parameters including lattice structure, fuel salt composition, solid moderator and P/D ratio (lattice pitch to channel diameter), based on our comprehensive screening for material and geometry of TMSR lattice [24], so as to have a breeding, sustainable and controllable TMSR. Table 1 presents the redesigned parameters for our TMSR core and lattice, and also Fig. 1 illustrates the redesigned TMSR core and lattice.

Table 1. Redesigned TMSR Core and Lattice

Core Parameters		Lattice Parameters	
Thermal Power, MW	2,400	Lattice Shape	Hexagon
Mass Flow rate, kg/s	9,000	Fuel Salt, Mole Percent	78%LiF-21.4%ThF_4-0.6%UF_4
Inlet /Outlet Temperature, K	893	Solid Moderator	BeO
Active Core Height, cm	400.	Channel Tube	SiC
Active Core Diameter, cm	～385	Lattice Pitch, cm	8.
Bottom/top Plenum, cm	30	SiC Tube Thickness, cm	0.1
Radial/Axial Reflector, cm	60	Larger Channel Diameter, cm	7.476
Fuel Channel Number	2,101	Medium Channel Diameter, cm	5.926
		Smaller Channel Diameter, cm	5.518

As for the redesigned TMSR core and lattice, the active core is formed of hexagonal BeO-moderated blocks, each one with a central SiC tube to form a fuel channel, through which the fuel salt flow. All the fuel channels are connected with bottom and top plenums, where the fuel salt is mixed with homogeneous properties. The core is still enveloped with graphite reflectors at bottom, top and periphery. The mixed fuel salt in top plenum flows out through hot leg pipes into primary heat exchangers (HX) and then is driven by salt pumps through cold leg pipes into the bottom plenum of the core. , see Fig. 1.

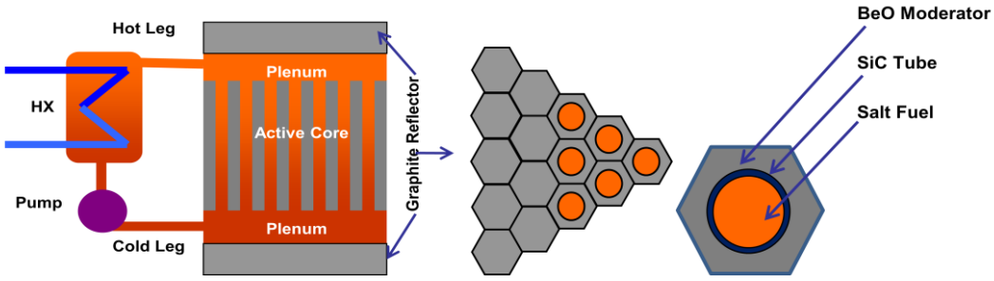

Fig. 1 Simplified TMSR System and The redesigned Lattice

2.2 System Modelling

The computer code we used in the paper is an in-house developed code system named SONG/TANG-MSR. SONG is a lattice code which employs MOC (Method of Characteristic) module to solve 2-dimensional/multi-group neutron transport equations. TANG-MSR is a special version of core code TANG which employs tightly coupled multi-physics models for solution of Neutronics and Thermal-hydraulics equations. In this paper, SONG is used to provide TANG-MSR with 8-group micro cross section for each TMSR isotope based on 293-group cross section library, which is generated from ENDF/B-VI.8; TANG-MSR is the main code used to simulate TMSR core.

Generally, the crucial models employed in TANG-MSR include Neutronics Model, Xsec Model, Precursor Transfer Model, T-H Model and Depletion Model. As we talked previously, since the liquid salt in MSR act as both fuel and coolant, and also due to the flowing precursors and online processing, the above models should be tightly coupled with each other as an integral multi-physics model, where Neutronics Model obtains spatial Macro-Xsec and precursor density from Xsec Model and Precursor Transfer Model respectively, and then provides neutron flux to Depletion Model and power density to T-H Model; T-H Model provides temperature, density and flowing velocity fields of fuel salt and/or moderator to Xsec Model and Precursor Transfer Model; Depletion Model provides spatial number density to Xsec Model; and also Xsec Model provides micro Xsec to Depletion Model and macro Xsec to Precursor Transfer Model and Neutronics Model. Fig.2 illustrated the tightly coupled multi-physics model employed in TANG-MSR code. The following is the brief description for these models.

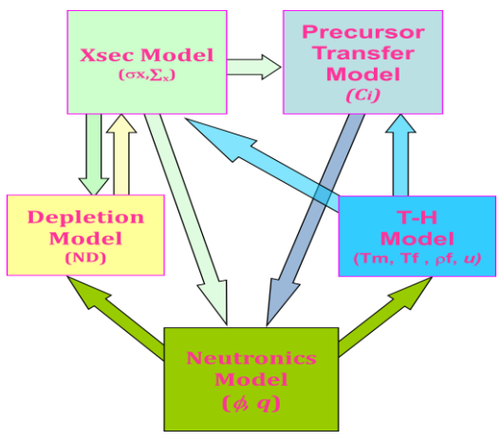

Fig.2 the Tightly Coupled Multi-physics Phenomena in TMSR

2.2.1 Neutronics Model

The standard 3-dimensional/multi-group neutron diffusion equations have been adopted to model the neutron balance in TMSR core:

$$\frac{1}{v_g}\frac{\partial}{\partial t}\phi_g(r,t) = D_g(r,t)\nabla^2\phi_g(r,t) - \Sigma_{rg}(r,t)\phi_g(r,t) + (1-\beta)\chi_{pg}\sum_{g'=1}^{G}\nu\Sigma_{fg'}(r,t)\phi_{g'}(r,t) + \sum_{\substack{g'=1 \\ g'\neq g}}^{G}\Sigma_{g'g}(r,t)\phi_{g'}(r,t) + \sum_{i=1}^{6}\chi_{ig}\lambda_i C_i(r,t) \quad (1)$$

Standard notation is used in above equations, The Nodal Expansion Method (NEM) is used to solve the space problem of the above diffusion equations [25]; the Universal Algorithm of Stiffness Confinement Method (UASCM) is used to solve time problem of the above diffusion equations [26]; the domain for equation (1) covers active core, top/bottom plenums, radial and top/bottom reflectors.

2.2.2 Precursor Transfer Model

The standard precursor balance equation is modified to take account of precursor evolution within the primary loop.

$$\frac{\partial}{\partial t}C_i(r,t) = \beta_i\sum_{g'=1}^{G}\nu\Sigma_{fg}(t)\phi_g(r,t) - \lambda_i C_i(r,t) - \nabla u C_i(r,t) \qquad i = 1,6 \quad (2)$$

Where $\nabla uC_i(r,t)$ is employed to model the lost delayed neutrons (precursors) caused by fuel salt flowing and u denotes the velocity of the fuel salt. The fuel velocity is assumed to be parallel to the axis of the reactor core. The Total Variation Diminishing (TVD) Scheme is used to solve the modified precursor equations. The domain for equation (2) covers whole primary loop including active core, top plenum, hot leg pipe, primary heat exchanger, cold leg pipe and bottom plenum.

2.2.3 Thermal-Hydraulic Model

Thermal-hydraulic model involves four parts: heat convection in fuel channel, heat conduction in moderator block, mass flow rate distribution among all fuel channels and fuel flowing through other components of primary loop.

Heat convection in each fuel channel is modelled individually with 1-D (parallel to the axis of the core) energy balance equation:

$$A_m\frac{\Delta z_n}{\Delta t}\rho_n'\left(h_n - h_n'\right) + G_m\left(h_n^{top} - h_n^{bot}\right) = 2\pi r_f\Delta z_n H_s\left(T_s - T_{f,n}\right) + \Delta z_n A_m q_{n,f} \quad (3)$$

Where, A_m -flowing area of fuel channel m, m^2;

ΔZ_n -height of axial mesh n, m;

Δt-time step size, second;

ρ'_n -bulk mass density (kg/m^3) of axial mesh at the beginning of given time step;

h'_n-bulk enthalpy (J/kg) of axial mesh at the beginning of given time step;

h_n-bulk enthalpy (J/kg) of axial mesh at end of given time step,

$h_n = \left(h_n^{top} + h_n^{bot}\right)/2$;

h_n^{top}, h_n^{bot} -enthalpy (J/kg) at top and bottom of axial mesh;

G_m -mass flow rate in channel, kg/s;

H_s-heat transfer coefficient at internal surface of fuel channel, W/m^2-K;

T_s -wall temperature of fuel channel, K;

$T_{f,n}$ -bulk temperature of fuel salt, K;

$q_{n,f}$ -power density deposited in fuel salt, (W/m^3);

The domain for equation (3) covers all fuel channels, bottom and top plenums, and also pipes and HXs, where the decay heat is releasing continuously.

Heat conduction in hexagonal moderator block can be approximately modelled with radial 1D heat conduction equation in a volumetrically equivalent annular moderator block, with assumption that the axial heat conduction is negligible and the radial heat conduction is isotropic.

$$\rho \cdot c_p \cdot \frac{dT}{dt} = k \cdot \frac{d^2T}{dr^2} + k \cdot \frac{dT}{dr} + q_m \qquad (4)$$

Where, ρ, c_p and k are mass density, specific heat capacity and heat conductivity of moderator respectively; q_m is the power density deposited in moderator block. Theoretically, the deposited power fraction depends on the lattice material, lattice pitch and P/D ratio, which has been calculated by Monte Carlo code and presented in Table 2. The domain for equation (4) is only the solid moderator block.

Table 2 Deposited Power Fractions in BeO Moderator with Different Lattice Design

P/D	P=4 cm	P=6 cm	P=8 cm	P=12 cm	P=16 cm	P=20 cm	P=24 cm
1.0	1.61%	1.60%	1.58%	1.56%	1.54%	1.52%	1.50%
1.2	3.97%	3.87%	3.78%	3.66%	3.53%	3.45%	3.36%
1.4	4.89%	4.72%	4.62%	4.47%	4.31%	4.19%	4.08%
1.6	5.46%	5.30%	5.16%	4.95%	4.81%	4.70%	4.60%
1.8	5.81%	5.66%	5.53%	5.35%	5.22%	5.07%	4.99%
2.1	6.23%	6.09%	5.96%	5.83%	5.68%	5.56%	5.46%
2.4	6.55%	6.43%	6.34%	6.17%	6.04%	5.95%	5.85%
2.8	6.89%	6.81%	6.71%	6.58%	6.47%	6.38%	6.32%
3.2	7.23%	7.12%	7.05%	6.95%	6.88%	6.76%	6.71%
3.6	7.55%	7.45%	7.41%	7.33%	7.24%	7.17%	7.12%
4.0	7.86%	7.79%	7.72%	7.65%	7.58%	7.53%	7.46%

Mass flow rate distribution among all fuel channels is estimated by solving momentum (pressure drop) balance equations. For a given TSMR core with M fuel channels, which are divided in N segments axially, the pressure drop for channel m can be expressed as:

$$\Delta P_m = \sum_{n=1}^{N} \frac{2 \cdot f \cdot \Delta Z_{m,n}}{d_m} \cdot \frac{G_m^2}{\rho_{m,n} \cdot A_m^2} \qquad (5)$$

Where f-friction coefficient;

d_m-diameter of channel m, m;

$\Delta Z_{m,n}$-mesh size for axial segment n of channel m, m;

Since all fuel channels are connected by bottom plenum and top plenum, the pressure drop in each fuel channel should be equal with each other, therefore,

$$\Delta P_m = \Delta P_{m+1} \qquad m = 1, M-1 \qquad (6)$$

$$\sqrt{\sum_{n=1}^{N} \frac{2 \cdot f \cdot \Delta Z_n}{\rho_{m,n} \cdot A_m^2 \cdot d_{f,m}}} \cdot G_m - \sqrt{\sum_{n=1}^{N} \frac{2 \cdot f \cdot \Delta Z_n}{\rho_{m+1,n} \cdot A_{m+1}^2 \cdot d_{f,m+1}}} \cdot G_{m+1} = 0 \qquad m = 1, M-1 \qquad (7)$$

The sum of mass flow rate in all fuel channels should be the total mass flow rate in core, which is a known quantity, that is:

$$\sum_{m=1}^{M} G_m = G_{core} \qquad (8)$$

Solving the equations combined with equation (7) and (8) can get the mass flow rate in each fuel channel of the active core.

Fuel flowing through other components of primary loop can be model with 1-D energy balance equation similar to equation (3), where the heat convection term may be omitted.

2.2.4 XSec Parameterization Model

Cross section parameterization model is the connection between Neutronics Model and Thermal-hydraulic Model. The Neutronics Model provides 3-D core neutron flux distribution and then the 3-D power density distribution to the Thermal-hydraulic Model, and then the moderator temperature T_m, fuel salt temperature T_f and mass density distribution ρ_f, and also the velocity u_f of the fuel salt in active core and other components of primary loop are produced by solving the Thermal-hydraulic Model. The moderator temperature T_m, fuel salt temperature T_f and mass density distribution ρ_f, are used to regenerate the local macro cross sections for each node within TMSR core, which are the equation coefficients of the Neutronics Model. This process is repeated till the distribution is converged.

Actually, the fuel salt temperature T_f and mass density ρ_f, are varied simultaneously for liquid fuel. The reason we select it as individual variable is to investigate fuel temperature coefficient and fuel density coefficient respectively.

The local macro cross sections for each node are modelled with following expression:

$$\sum_x(T_m,T_f,\rho_f)=\sum N(\rho_f)\cdot\sigma_x(T_m,T_f,\rho_f) \qquad x=D,t,f,gg',etc \tag{9}$$

The standard notation is used in above equation, where the micro cross section $\sigma(T_m, T_f, \rho_f)$ is interpolated from a prepared cross section table generated by lattice code SONG.

2.2.5 Depletion Model

The classical Bateman equation to track the evolution of isotope i is as follows:

$$\frac{dN_i^{ref}}{dt}=\sum_j\gamma_{j,i}\sigma_{f,j}N_j^{ref}\phi+\sigma_{c,i-1}N_{i-1}^{ref}\phi+\sum_k\lambda_{k,i}N_k^{ref}-\sigma_{a,i}N_i^{ref}\phi-\lambda_iN_i^{ref} \tag{10}$$

Standard notation is used in above equation. Since the fuel salt is flowing in TMSR, we could not solve the above equation like those reactors employing solid fuel. Here we can think the whole primary system as a unique depletion volume. Therefore, the reaction rates $\sigma_x\phi$ in equation (10) should be the core averaged values.

Since the fuel in core may have neutron incurred reactions and decay behaviour, whereas the fuel out of core may only have decay behaviour, we need a time sharing fraction α to take into account the above phenomena, which is defined as:

$$\alpha=\frac{t_{in}}{t_{in}+t_{out}}=\frac{t_{in}}{t_{circ}} \tag{11}$$

Where t_{in} is travelling time of flowing fuel in core, t_{out} is travelling time of flowing fuel out of the core, and t_{circ} is travelling time of flowing fuel through one circulation of the primary loop. The travelling time for flowing fuel at each stop (core, plenums, pipes and HX, etc.) of the primary loop is estimated with the free volume of each component and the local volumetric flow rate,

$$t_i=\frac{V_i}{m_i}=\frac{V_i\rho_i}{G_i},\ i=\text{core, plenum, pipe and HX} \tag{12}$$

Where, V_i-free volume of component i, m^3;

m_i--local volumetric flow rate of component i, m^3/s;

ρ_i--local mass density of component i, kg/m^3;

G_i--local mass flow rate of component i, kg/s;

By using time sharing fraction α, the Bateman equation accounting of flowing fuel salt can be revised as follows:

$$\frac{dN_i^{ref}}{dt}=\alpha\sum_j\gamma_{j,i}\sigma_{f,j}N_j^{ref}\phi+\alpha\sigma_{c,i-1}N_{i-1}^{ref}\phi+\sum_k\lambda_{k,i}N_k^{ref}-\alpha\sigma_{a,i}N_i^{ref}\phi-\lambda_iN_i^{ref} \tag{13}$$

Another important feature of MSR is the online fuel processing, which involves fission gas (Kr and Xe) removed by gas stripping process, noble metal (Ru, Rh, Pd, Ag, etc.) plated out on structure surface, and also the online feeding and extracting of the fuel salt. The above processes shall directly disturb the isotopes balance in MSR system and should be appropriately modelled.

As for the fission gas and noble metal, we introduced an extracting constant to model the effect of related processing. Similar as the definition of decay constant, the extracting constant is defined as:

$$\lambda_{ex} = \frac{\ln 2}{t_{half}} \qquad (14)$$

The above t_{half} is time consumed to extract half of the element by using specific process, which can be tested out of core for given process. Then the Bateman equation accounting of online separation of fission gas and noble metal can be written as follows:

$$\frac{dN_i^{ref}}{dt} = \alpha \sum_j \gamma_{j,i}\sigma_{f,j}N_j^{ref}\phi + \alpha\sigma_{c,i-1}N_{i-1}^{ref}\phi + \sum_k \lambda_{k,i}N_k^{ref} - \alpha\sigma_{a,i}N_i^{ref}\phi - \lambda_i N_i^{ref} - \lambda_{ex,i}N_i^{ref} \qquad (15)$$

Online continuous feeding and extracting of fuel salt are modelled with elimination rate and producing rate respectively. Assumed that the mass flow rates for feeding and extracting are G_f and G_e respectively and the total inventory of fuel salt in primary loop is Q, then the Bateman equation accounting of continuous feeding and extracting of fuel salt can be written as:

$$\frac{dN_i^{ref}}{dt} = \alpha \sum_j \gamma_{j,i}\sigma_{f,j}N_j^{ref}\phi + \alpha\sigma_{c,i-1}N_{i-1}^{ref}\phi + \sum_k \lambda_{k,i}N_k^{ref} - \alpha\sigma_{a,i}N_i^{ref}\phi - \lambda_i N_i^{ref} - \lambda_{ex,i}N_i^{ref} - \frac{G_e}{Q}N_i^{ref} + \frac{G_f}{Q}N_i^{ref} \qquad (16)$$

Equation (16) is the general Bateman equation for MSR system and is solved with Matrix Exponent Method in TANG-MSR.

3. Simulated Results and Discussion

The general design parameters for the TMSR we simulated are listed in Table 1. Specifically, the core is composed of 3 regions; The core periphery is loaded with larger diameter channel (276 blocks), and the medium diameter channel blocks (163) are loaded in the central region, rest of the core are composed of smaller diameter blocks (1,650) so as to form so-called fire ring. The core is configured with 12 Ag-In-Cd control rods to provide reactivity control. Layout of the radial core is presented in Fig. 3. The configuration of these fuel channels is the balance of the radial power distribution, extra reactivity and the Breeding Ratio.

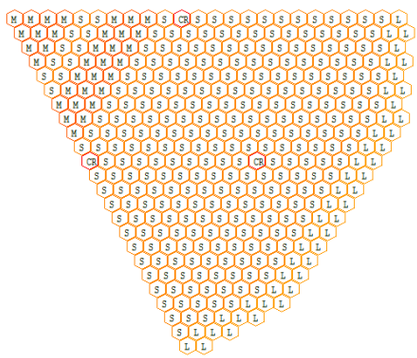

Fig. 3 Radial Core Layout of the Simulated TMSR

The following are the simulated results for normal depletion operation, steady state and transient respectively.

3.1 Depletion Operation

TMSR is assumed to operate with online fission gas separation, noble metal separation, and continuous online feeding and extracting. As for the reference core, the designed feeding volumetric flow rate is 100cm^3/s with the fresh fuel salt defined in Table 1. As a result of the volume control, the extracting flow rate should be the same as feeding. As we talked above, the fission gas separation and noble metal separation are modelled with extracting constants, whose

half time are assumed with 120 seconds and 300 seconds for the time being respectively. The core criticality is maintained with control rods insertion.

Fig.4 shows the critical rods position evolution with the depletion time. It can be seen from Fig.4 that the control rods are withdrawn at the early stage to compensate the accumulation of fission products and shall reach equilibrium position around 20 hot full power days (HFPDs). The Breeding Ratio with classical definition (ratio of capture rate of fertile to absorption rate of fissile) is also presented with more than 1.1 in Fig. 4, which is quite better than that in original MSBR of ORNL.

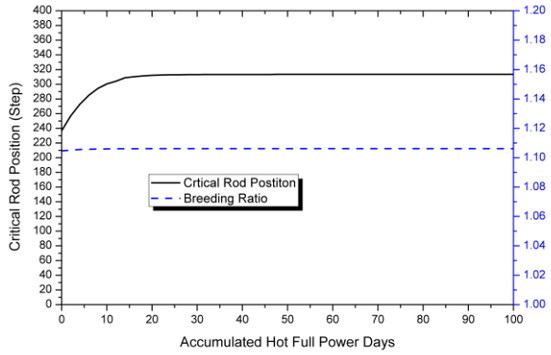

Fig. 4 Critical Rod Position and Breeding Ratio Evolution with Normal Operation

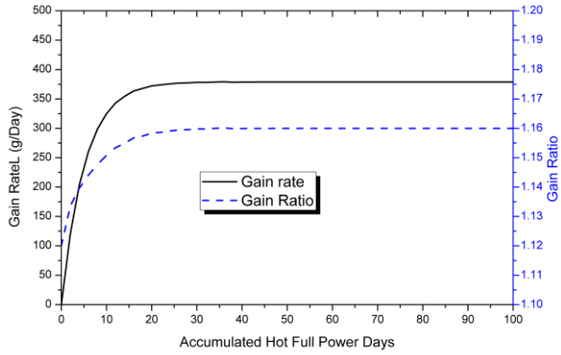

Fig. 5 Gain ratio and Gain Rate Evolution with Normal Operation

Fig.5 presents the Gain Ratio and Gain Rate for the reference core, both of which are defined based on the feeding mass flow and extracting mass flow. The feeding mass flow rate of ^{233}U (g/s)-FU3-can be got from the feeding fuel salt directly, and the extracting mass flow rates of ^{233}U and ^{233}Pa (g/s) -EU3 and EPa3-can be estimated based on the depletion solutions, with the assumption that all extracted ^{233}Pa shall decay into ^{233}U, we define Gain Rate = EPa3+EU3-FU3 and Gain Ratio = EPa3/(FU3-EU3). It can be seen from Fig.4 and Fig. 5 that the Gain Ratio is a little bit bigger than Breeding Ratio and the Gain Rate of ^{233}U for reference core is around 370 g/day, which means the Doubling Time for the reference core is about 20 years.

3.2 Steady-state

Fig.6 shows the axially averaged radial power distribution for reference core. Due to the effect of graphite reflector, the core periphery presents higher power sharing, even though the larger diameter channel has been loaded on the periphery, which has the lowest reactivity. Fig.7 gives the temperature distribution at the core outlet, where the coloured round identifies the fuel temperature and the coloured background shows the moderator temperature distribution.

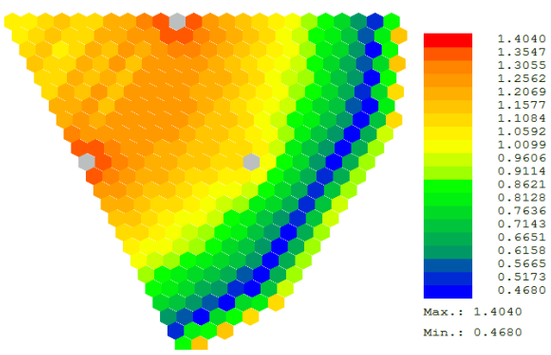

Fig. 6 Radial Power Distribution

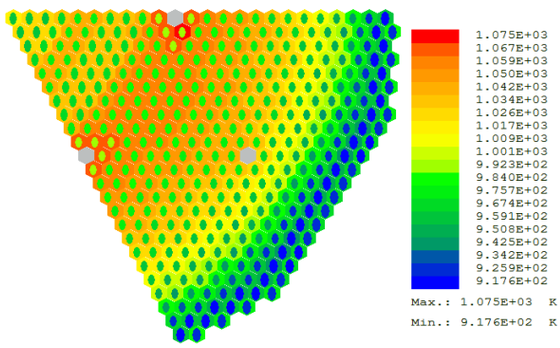

Fig.7 Outlet Temperature Distribution

Fig.8 and Fig.9 present the mass flow rate distribution and the outlet velocity distribution respectively. Obviously, channel diameter is the dominated factor to the mass flow rate distribution and outlet velocity. Furthermore, the power sharing also has influence on the outlet velocity, even though the channel diameters are the same.

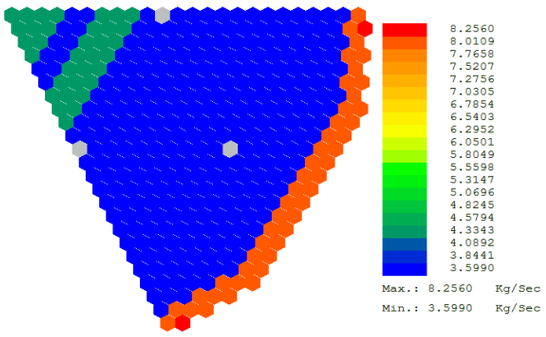

Fig. 8 Mass Flow Rate Distribution

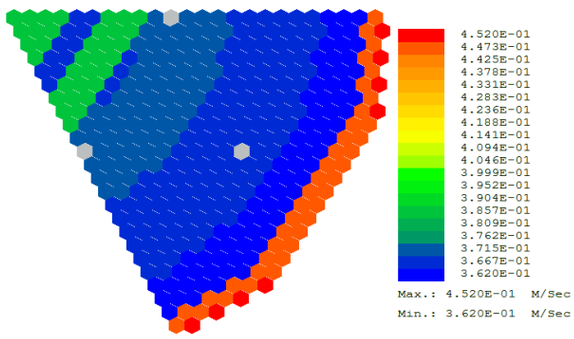

Fig. 9 Outlet Velocity Distribution

Fig.10 shows the Doppler only temperature coefficient and fuel temperature (density associated) coefficient vs. the fuel temperature in initial core and depleted core. There is no obvious difference for these temperature coefficients between initial core and equilibrium core in Fig.10 and the fuel temperature (density associated) coefficient is less negative than the Doppler only temperature coefficient due to the positive fuel density effect in sub-moderated lattice. Even so, the fuel temperature (density associated) is negative enough to overcome the positive moderator effect [22, 23] and finally provides an enough negative power coefficient, which is presented in Fig.11, and it also eventually guarantees that the reference TMSR core is safe and controllable.

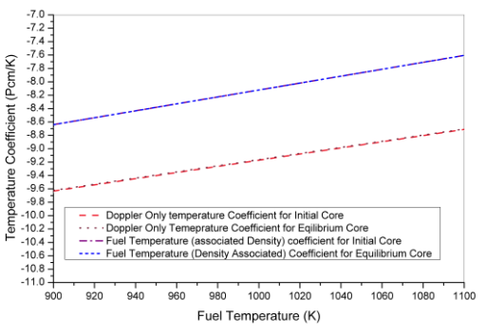

Fig. 10 Fuel Temperature Coefficient vs. Fuel Temperature

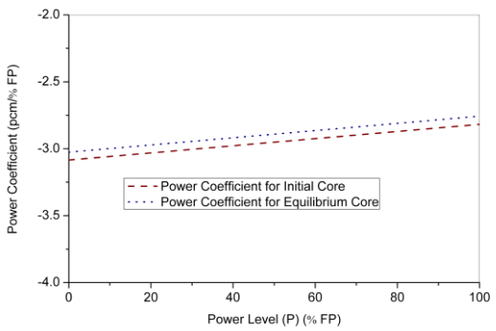

Fig. 11 Power Coefficient vs. Power level

The flowing fuel salt in TMSR causes loss of the delayed neutron precursors and associated delayed neutrons. Fig.12 shows the comparison of 6-group precursor density distribution in the view of axial section for the cores with and without fuel flowing, where the dash line in each picture identifies the axial central-line of core. As for the core without fuel flowing, see Fig.12 (b), the precursor density is mainly concentrated in the middle plane of the core, actually a little bit bias to bottom due to the tilted axial power shape as shown in Fig.13; while in the core with fuel flowing, see Fig.12 (a), the dense region is significantly moved to top of the core especially for the longer lifetime groups (g1, g2, g3 and g4), but there is slight influence on the shorter lifetime groups (g5 and g6). Therefore, we can understand that the reactivity loss caused by flowing fuel salt is mainly due to the loss of longer lifetime precursors, and also it is clear that the bigger the flowing velocity is, the larger the reactivity loss is. Fig.14 just presents the reactivity loss vs. the core averaged flowing velocity. As the velocity in reference core is around 0.38 m/s, the reactivity loss caused by flowing fuel salt is around 100 pcm in reference core.

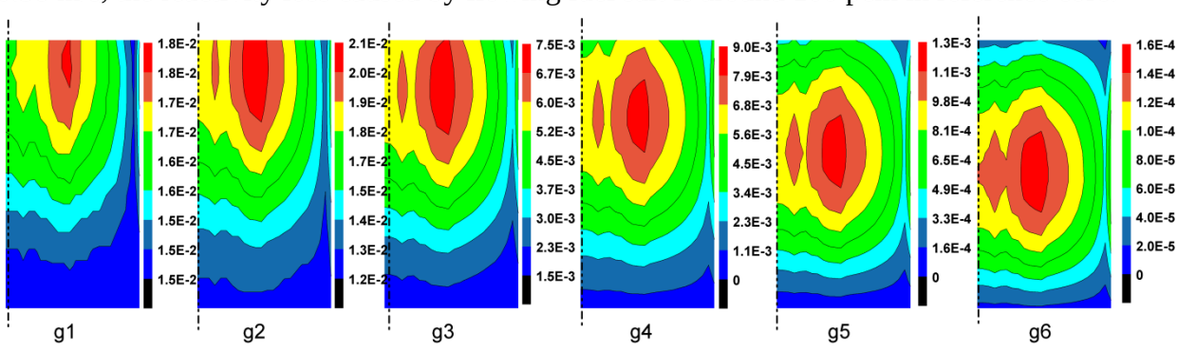

(a) Precursor Density with Fuel Flowing

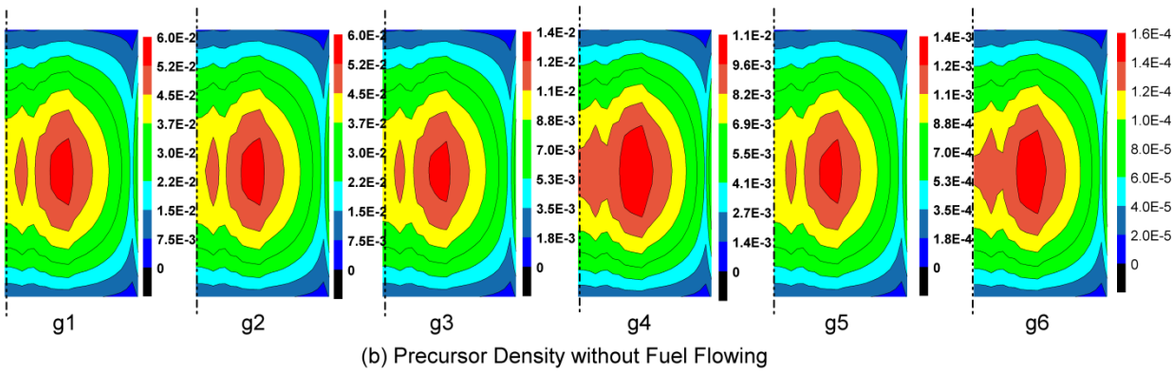

Fig. 12 Axial Section View of Precursor Density Distribution for the core with and without Fuel Flowing

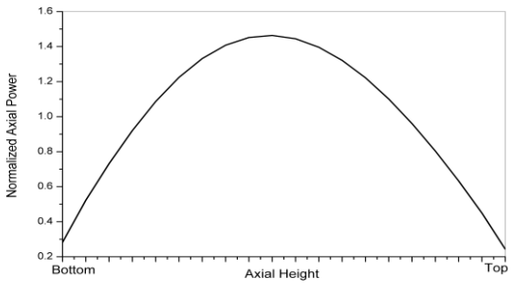

Fig. 13 Axial Power Distribution

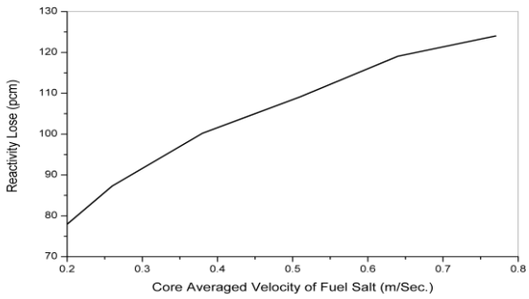

Fig. 14 Reactivity Loss vs. Fuel Velocity

3.3 Transient

TMSR operation is mainly controlled by control rods during start-up, power operation and shut-down. Fig.15 and Fig.16 present the simulation results for nuclear power and temperatures response to the control rods withdrawal during start-up transient. The process is divided into 3 stages; and the time duration for each stage is 150 seconds. At the beginning of each stage, the control rods are withdrawn with speed of 2steps/s totally for 12 steps (1cm/step). It can be seen from Fig.15 and Fig.16 that the core can be stably started up from hot zero power to near hot full power.

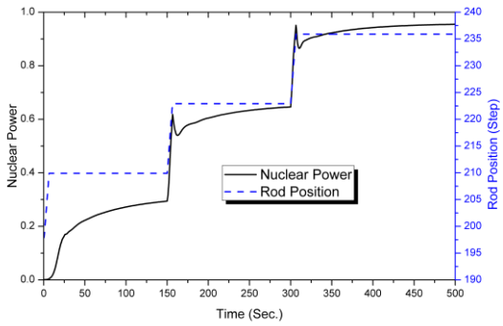

Fig. 15 Nuclear Power Response to Control Rod Withdrawal during Startup

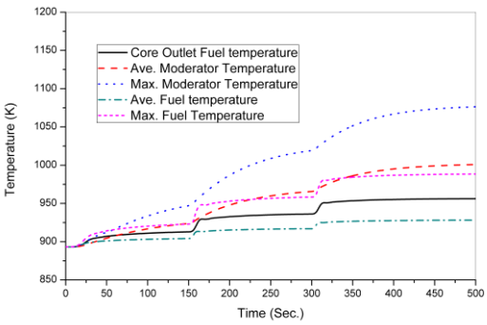

Fig. 16 Temperature Response to Control Rod Withdrawal during Startup

As we talked above, flowing fuel salt results in reactivity loss, therefore, the variation of pumping rate (i.e. mass flow rate in core) during normal operation shall cause corresponded reactivity insertion for operating core. Fig.17 and Fig.18 present the power and temperature response to mass flow rate during the transient of pump speed down; Fig.19 and Fig.20 present the power and temperature response to mass flow rate during the transient of pump speed up. For both cases, the initial core is operating with nominal hot full power.

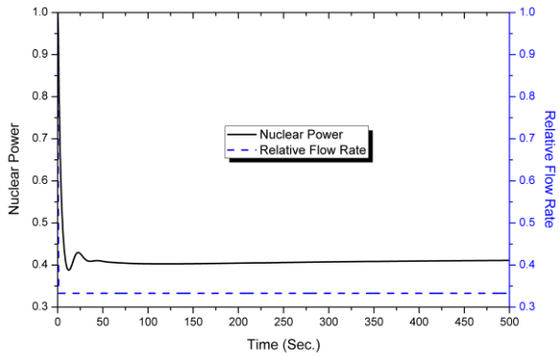

Fig. 17 Nuclear Power Response to Flow Rate during Pump Speed down

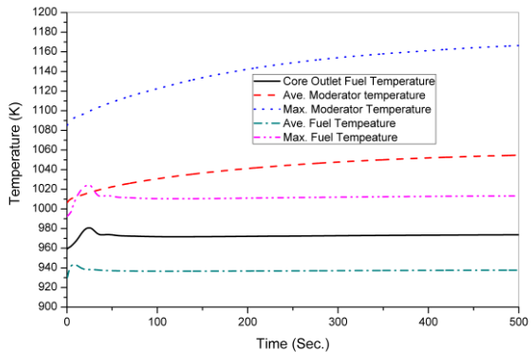

Fig. 18 Temperature Response to Flow Rate during Pump Speed down

As for the pump speed down, the flow rate is assumed to decrease to 33.3% of the rated value within 1 second. It can be seen from Fig.17 that the core nuclear power is quickly decreased to ~40% HFP. The decrease of the flow rate means that part of the lost delayed neutron shall come back to active core and cause positive reactivity insertion. On the other hand, the decrease of the flow rate shall also cause the increase of fuel temperature in active core and cause negative reactivity insertion; Thanks to the enough negative fuel temperature coefficient, the final net reactivity insertion is negative, therefore, the core nuclear power is quickly decreased. This feature is crucial in TMSR for the possible pump malfunction events. Fig.18 shows that the peaking temperature in active core is still within safe scope, as the maximum working temperature for SiC is over 1,800K and the molten point for BeO is around 3,000K.

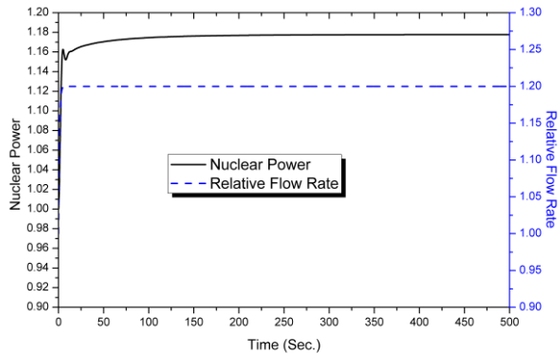

Fig. 19 Nuclear Power Response to Flow Rate during Pump Speed up

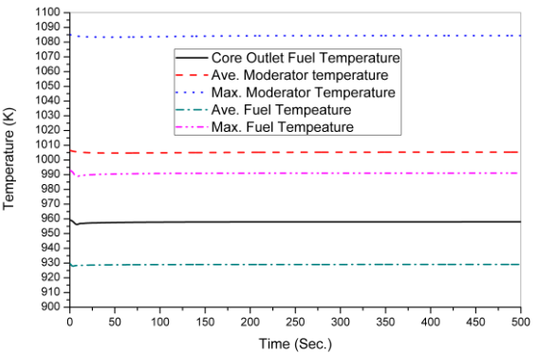

Fig. 20 Temperature Response to Flow Rate during Pump Speed up

Pumping speed up is another situation possibly caused by internal or external incidents. As an opposite of pumping speed down, it shall cause positive net reactivity insertion. It can be seen from Fig.19 that the nuclear power is quickly increased and finally got stable around 117% HFP when the mass flow rate is increased to 120% of rated value within 2 seconds. However, the variation of temperature shown in Fig.20 is not so significant, even slightly decreased. The reason is that the increased mass flow rate causes decrease of fuel enthalpy rise (i.e. temperature rise) in active core and also increase of cooling effect to the solid moderator. Therefore, the core under the condition of pump speed up is safe.

4. Conclusion

A tightly coupled multi-physics model for MSR has been developed and employed in an in-house developed computer code TANG-MSR, which has been used to simulate and redesign for our new concept of TMSR. The presented simulation results demonstrate that the models employed in TANG-MSR can capture major physics phenomena in MSR and the redesigned TMSR has excellent performance of safety and sustainability.

5. Acknowledgments

This work is supported by National Science Foundation of China (Grant No. Project: 91326201).

6. References

[1] Generation IV International Forum (2002), A Technology Roadmap for Generation IV Nuclear Energy Systems, Report GIF-002-00.

[2] D. Lecarpentier and J. Vergnes (2002), The AMSTER (Actinide Molten Salt TransmutER) Concept, Nucl. Eng. and Des. 216, 43-67.

[3] Mitachi, K., Yamamoto, T., Yoshioka, R., 2007. Three-region core design for 200 MWe molten-salt reactor with thorium-uranium fuel. Nuclear Technology 158, 348–357.

[4] L. Mathieu et al (2003), Thorium Molten Salt Reactor: from High Breeding to Simplified Reprocessing, GLOBAL 2003, New-Orleans, USA, 16-20 November.

[5] L.Mathieu et al, Proposition for a Very Simple Thorium Molten Salt Reactor, Global Conference, Tsukuba, Japan (2005).

[6] L. Mathieu, D. Heuer et al, The Thorium Molten Salt Reactor: Moving on from the MSBR, Prog. in Nucl. En., vol 48, pp. 664-679 (2006).

[7] R.C. Robertson, ed., Conceptual Design Study of a Single Fluid Molten Salt Breeder Reactor, ORNL-4541(1971).

[8] M.W.Rothental, P.N.Haubenreich, R.B.Briggs, The Development Status of Molten-Salt Breeder Reactors, ORNL-4812(1972).

[9] Lecarpentier, D., Carpentier, V., A neutronics program for critical and nonequilibrium study of mobile fuel reactors: the Cinsf1D code. Nucl. Sci. Eng. 143, 33–46, 2003..

[10] Wang, S., Rineiski, A., Maschek, W.. Molten salt related extensions of the SIMMER-III code and its application for a burner reactor. Nucl. Eng. Des. 236, 1580–1588, 2006.

[11] Yamamoto, T., Mitachi, K., Ikeuchi, K., Suzuki, T.. Transient characteristics of small molten salt reactor during blockage accident. Heat Transfer Asian Res. 35, 434–450, 2006.

[12] Yamamoto, T., Mitachi, K., Suzuki, T.. Steady state analysis of small molten salt reactor. JSME Int. J. Ser. B 48 (3), 610–717, 2005.

[13] Krepel, J., Rohde, U., Grundmann, U., Weiss, F.P.. DYN3D-MSR spatial dynamics code for molten salt reactors. Ann. Nucl. Energy 34, 449–462, 2007.

[14] Nicolino, C., Lapenta, G., Dulla, S., Ravetto, P.. Coupled dynamics in the physics of molten salt reactors. Ann. Nucl. Energy 35, 314–322, 2008.

[15] Kópházi, J., Lathouwers, D., Kloosterman, J.L.. Development of a threedimensional time-dependent calculation scheme for molten salt reactors and validation of the measurement data of the molten salt reactor experiment. Nucl. Sci. Eng. 163, 118–131, 2009.

[16] Zhang, D.L., Qiu, S.Z., Su, G.H., Liu, C.L., Qian, L.B.. Analysis on the neutron kinetics for a molten salt reactor. Prog. Nucl. Energy 51, 624–636, 2009.

[17] Zhang, D.L., Qiu, S.Z., Su, G.H.. Development of a safety analysis code for molten salt reactors. Nucl. Eng. Des. 239, 2778–2785, 2009.

[18] Zhang, D.L., Qiu, S.Z., Su, G.H., Liu, C.L.. Development of a steady state analysis code for a molten salt reactor. Ann. Nucl. Energy 36, 590–603, 2009.

[19] Antonio Cammi, Valentino Di Marcello, Lelio Luzzi, Vito Memoli, Marco Enrico Ricotti. A multi-physics modelling approach to the dynamics of Molten Salt Reactors, Annals of Nuclear Energy 38, 1356–1372, 2011

[20] Jozsef Kophazi, Danny Lathouwers, Jan Leen Kloosterman, Sandor Feher, Three-dimensional space and time-dependent analysis of molten salt reactors, PHYSOR 2006–Advances in Nuclear Analysis and Simulation, Vancouver, BC (Canada), Sep 10-14, 2006.

[21] Karoly Nagy, Dynamics and Fuel Cycle Analysis of a Graphite Moderated Molten Salt Reactor, Master Thesis, Budapest University of Technology and Economics, 2012.

[22] NUTTIN, A., et al, Potential of Thorium molten salt reactors: detailed calculations and concept evolution with a view to large scale production energy, Progress in nuclear energy, 46, (2004), 77.

[23] Shengyi Si, Qichang Chen, Hua Bei, Jinkun Zhao, New Exploration on TMSR: The Lattice Optimization, Proceedings of the 2014 22nd International Conference on Nuclear Engineering, ICONE22, July 7-11, 2014, Prague, Czech Republic.

[24] Shengyi Si, Qichang Chen, Hua Bei, Jinkun Zhao, New Exploration on TMSR: Redesign of the TMSR Lattice, Proceedings of the 2016 24nd International Conference on Nuclear Engineering, ICONE24, to be released soon.

[25] Shengyi Si, 3D coarse mesh NEM embedded with 2D fine mesh NDOM for PWR core analysis, PHYSOR 2010-Advances in Reactor Physics to Power the Nuclear Renaissance，Pittsburgh, Pennsylvania, USA, May 9-14, 2010..

[26] Shengyi Si, Algorithm development and verification of UASCM for multi-dimension and multi-group neutron kinetics model, PHYSOR 2012–Advances in Reactor Physics – Linking Research, Industry, and Education Knoxville, Tennessee, USA, April 15-20, 2012.